

# Coexistence of Bound and Virtual-bound States in Shallow-core to Valence Spectroscopies

Subhra Sen Gupta,<sup>1,\*</sup> J. A. Bradley,<sup>2</sup> M. W. Haverkort,<sup>3</sup> G. T. Seidler,<sup>2</sup> A. Tanaka,<sup>4</sup> and G. A. Sawatzky<sup>1</sup>

<sup>1</sup>*Department of Physics and Astronomy, University of British Columbia, Vancouver, BC V6T 1Z1, Canada.*

<sup>2</sup>*Department of Physics, University of Washington, Seattle, Washington 98105, USA.*

<sup>3</sup>*Max Planck Institute for Solid State Research, Heisenbergstraße 1, D-70569 Stuttgart, Germany.*

<sup>4</sup>*Department of Quantum Matter, ADMS, Hiroshima University, Higashi-Hiroshima 739-8530, Japan.*

(Dated: December 9, 2018)

We develop the theory for shallow-core to valence excitations when the multiplet spread is larger than the core-hole attraction, *e.g.*, if the core and valence orbitals have the same principal quantum number. This results in a cross-over from bound to virtual-bound excited states with increasing energy and in large differences between dipole and high-order multipole transitions, as observed in inelastic x-ray scattering. The theory is important to obtain ground state information from x-ray spectroscopies of strongly correlated transition metal, rare-earth and actinide systems.

PACS numbers: 78.70.Ck, 78.70.Dm, 78.20.Bh, 78.47.da

The actinides and their compounds are attracting serious attention from the condensed matter community due to their exotic properties [1]. Examples of these are the extremely rich phase diagram of Plutonium [2] and the unsolved “hidden order” transition [3] in URu<sub>2</sub>Si<sub>2</sub>. Their properties interpolate between more itinerant 3*d* transition metal (TM) systems and more localized 4*d* TM compounds [4], and exhibit strong interplay between spin, charge, orbital, and lattice degrees of freedom. Thus, versatile experimental techniques are needed to unravel the physics operative in these systems. Core-level spectroscopies, like x-ray absorption spectroscopy (XAS), have been extremely successful in providing information regarding the ground state of TM and rare-earth (RE) systems, relying largely on theoretical interpretations based on local correlated models with full multiplet effects [5] and atomic selection rules.

The success of such local multiplet models relies strongly on two facts : (1) their electronic structure is largely governed by local correlation physics and point group symmetry, and (2) the final state core-hole strongly binds the extra *d* or *f* electron, so that *all* core-valence multiplets (CVM) form *excitonic bound states*. However, core-valence excitations within the *same principal quantum number (n)-shell*, like 4*d*-4*f* transitions in RE, or 5*d*-5*f* transitions in the actinides, pose a problem because the CVM spread is  $\sim 20$ -25 eV, often much larger than the average core-hole valence-electron attractive potential ( $Q$ ) itself! This places higher lying terms up in the conduction band, ‘autoionizing’ the extra *f* electron. This mixing with continua gives rise to very broad, virtual-bound (V-B) *Fano-resonances* [6], that cannot be interpreted in terms of local models. We note that this is an additional effect to those involving the decay of the core-hole itself, which have been elegantly described [7, 8] for these giant dipole resonances (GDR) [10].

The strong hybridization of the 5*f* electrons with conduction band states requires detailed information about

interatomic interactions and band structure effects, ruling out the usefulness of atomistic models. In this paper, we emphasize that the structure of core-level excitations within the same *n*-shell, is fundamentally different from that between different *n*-shells, with the example of the 5*d*→5*f non-resonant inelastic x-ray scattering* (NIXS) in the actinides. We also show that the high-multipole (HM) transitions in NIXS to strongly bound CVM states [11], unlike the dipole restricted transitions in XAS and EELS, can still be treated within local models, but with strongly renormalized parameters, due to very large *configuration interaction* (CI) in the final state.

Unlike dipole restricted XAS, NIXS can access transitions involving high-order multipoles as exemplified by the observation of *d-d* transitions in TM compounds [12, 13]. It also gives us more information of what the true ground state of the system actually was, even for dipole-allowed transitions [11, 14]. NIXS uses the first order scattering, off-resonance, due to the  $(e^2/2mc^2)\vec{A}\cdot\vec{A}$  term in the light-matter coupling [15]. The corresponding double differential cross section is given by [15] the *Thompson scattering cross-section*, times the material dependent *dynamical structure factor* :

$$S(\vec{q}, \omega) = \sum_f |\langle f | e^{i\vec{q}\cdot\vec{r}} | i \rangle|^2 \delta(E_f - E_i - \hbar\omega) \quad (1)$$

where,  $\vec{q}=\vec{k}_i-\vec{k}_f$  is the *photon momentum transfer*, and  $\hbar\omega=\hbar\omega_i-\hbar\omega_f$  is the *energy loss*. The transition operator can be multipole expanded [13] as :  $e^{i\vec{q}\cdot\vec{r}} = \sum_{l=0}^{\infty} \sum_{m=-l}^l i^l (2l+1) j_l(qr) C_m^{(l)*}(\theta_{\vec{q}}, \phi_{\vec{q}}) C_m^{(l)}(\theta_{\vec{r}}, \phi_{\vec{r}})$ , where,  $j_l(qr)$  are spherical Bessel functions, while  $C_m^{(l)}(\theta, \phi)$  are renormalized spherical harmonics, both of order *l*. Only terms with  $|l_f - l_i| \leq l \leq (l_f + l_i)$  and  $(l + l_i + l_f)$  *even*, survive in the infinite sum.

As a relevant illustration we show, in the *inset-1* to Fig. 1(a), the radial transition probabilities for the various allowed channels in the 5*d*→5*f* NIXS of the Th<sup>4+</sup>

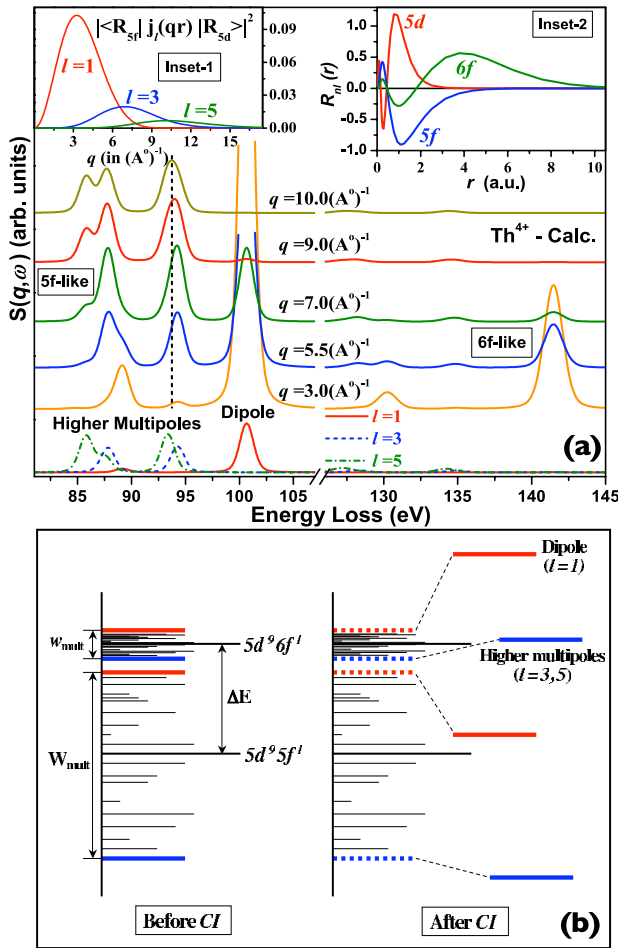


FIG. 1: (color online) (a) The variation of the radial transition probabilities with  $q$ , for the three component channels,  $l = 1$  (dipole), 3 (octupole) and 5 (triacontadipole) (inset-1); plots of the  $5d$ ,  $5f$  and  $6f$  atomic H-F radial wavefunctions for  $\text{Th}^{4+}$  (inset-2); and calculated NIXS ( $S(q, \omega)$ ) for  $\text{Th}^{4+}$  ( $5f^0$ ) including final-state CI with the  $6f$  level, for 60% of atomic  $CI(5f-6f)$  values (main). Both the  $5f$ -like and  $6f$ -like regions are shown. The bare component ( $l=1, 3, 5$ ) spectra (not to scale) are shown at the bottom. (b) Schematic illustrating the high sensitivity of the dipole term vis-a-vis the HM terms, to the strongly term-dependent CI with the  $6f$ .

( $5f^0$ ) system (relevant for  $\text{ThO}_2$ ), plotted against  $q$ , as obtained using Cowan’s atomic Hartree-Fock (H-F) code [16]. From the selection rules, this transition has allowed channels for the *dipole* ( $l=1$ ), *octupole* ( $l=3$ ) and the *triacontadipole* ( $l=5$ ) sectors. The  $q$  and  $l$  dependence of the transition probabilities can be understood from the properties of  $j_l(qr)$ , as described by Haverkort *et al.* [13].

While, details of the experimental data are discussed in the experimental paper [17], here we briefly remind the reader of the key results obtained therein, *viz.*: (i) NIXS data for actinides show the dichotomy that HM features are sharp and excitonic, while the Fano-like asymmetric [6] dipole feature is spread out over a very large energy range; (ii) in stark contrast, the calculated low- $q$

dipolar NIXS spectra are much sharper, intense and similar to the lower energy HM multiplets; (iii) in order to obtain reasonable agreement with experimental spectra in terms of the peak positions, we needed to drastically scale down the  $5d$ - $5f$  Coulomb and exchange Slater integrals ( $F_{df}^k, G_{df}^k$ ), to 60% ( $\text{ThO}_2$ ) or 50% ( $\text{UO}_2$ ) of their atomic H-F values! This is hard to justify for these rather atomic-like  $5f$  wavefunctions [18, 19]. In passing, we note that the dichotomy, discussed in (i) above, is also observed in the  $4d \rightarrow 4f$  NIXS of the RE [11] and the  $3p \rightarrow 3d$  NIXS of TM compounds [14], and between the “doubly forbidden” pre-edge peak and the GDR, in the  $\text{O}_{45}$  XAS of actinides [1], showing that this is a generic feature for shallow core-valence transitions within the *same*  $n$ -shell.

To understand the origin of the apparent large reductions in the Slater integrals, we plot in the *inset-2* of Fig. 1(a), the  $5d$ ,  $5f$  and the  $6f$  radial wavefunctions, obtained from an atomic H-F calculation for  $\text{ThO}_2$  ( $\text{Th}^{4+}$ , ground configuration  $5f^0$ ). The  $5d$  and  $5f$  orbitals (same  $n$ -shell) overlap very strongly, which accounts for the large values of the atomic ( $F_{df}^k, G_{df}^k$ ) integrals. In contrast, the more diffuse  $6f$  orbital, with an additional radial node, overlaps only weakly with the  $5d$ . Hence, a final state (CI) between  $5d^9 5f^1$  and  $5d^9 6f^1$ , via the  $CI(5f-6f)$  matrix elements [20], would effectively expand the radial part of the  $5f$  wavefunction, reducing the  $5d$ - $5f$  Slater integrals. Now, the mixing depends also on the energy separation,  $\Delta E$ , between the center-of-gravities (CG) of configurations involved, which is smaller in the actinides, than between  $4d^9 4f^1$  and  $4d^9 5f^1$  in the RE. This results in a strong multiplet-dependent CI, because the multiplet splitting in  $5d^9 5f^1$  is much larger than that in  $5d^9 6f^1$ , as shown schematically in Fig. 1(b). To illustrate this point, the NIXS spectra for  $\text{ThO}_2$  ( $\text{Th}^{4+}$ ) are calculated (using the XTLS8.3 code [21]) on the basis of the above model, as a coherent combination of the transitions  $5f^0 \rightarrow 5d^9 5f^1$  and  $5f^0 \rightarrow 5d^9 6f^1$  [22]. Here we leave the ( $F_{df}^k, G_{df}^k$ ) integrals unaltered at their atomic H-F values, while the scaling of  $CI(5f-6f)$  is varied to obtain agreement with experimental peak positions. This presents a more natural and physical mechanism for understanding the reduced multiplet spread observed experimentally. The fact that we need to scale the CI integrals merely indicates that the band-like  $6f$  state is poorly approximated by the atomic H-F calculations, and that CI with numerous other states is neglected here. The full  $q$ -dependent spectra, at the optimized 60% scaling of  $CI(5f-6f)$  (Fig. 1(a)), is spread over a wide energy range and consists of  $5f$ -like and  $6f$ -like regions (marked in the figure), although most of the spectral weight lies in the  $5f$ -like region due to dominance of radial matrix elements. The CI serves to reduce the  $5d$ - $5f$  multiplet spread considerably (while enhancing the  $5d$ - $6f$  spread), especially pushing the dipole peak close to the HM peaks, in good agreement with experiments [17]. Also the component spectra for the  $l=1, 3, 5$  channels plotted at the

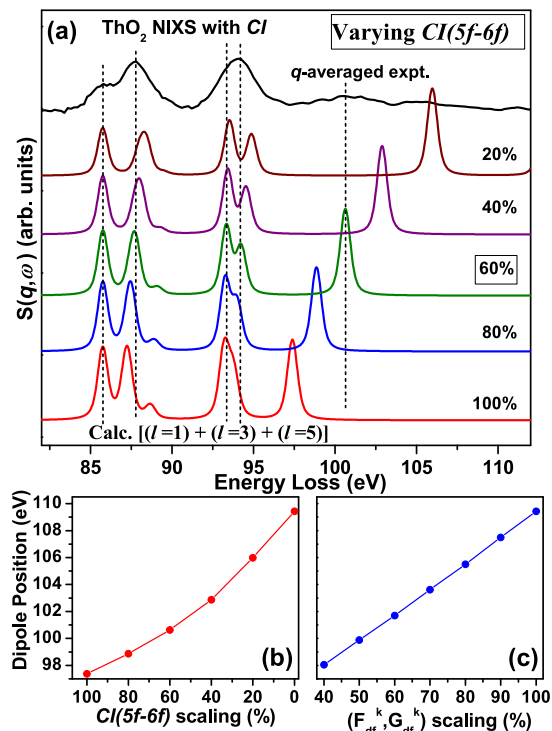


FIG. 2: (*color online*) (a) Experimental  $q$ -averaged NIXS for  $\text{ThO}_2$ , compared with the component ( $l=1, 3, 5$ ) summed calculated spectra for atomic values of  $(F_{df}^k, G_{df}^k)$ , and the  $CI(5f-6f)$  varied from a scaling of 20% to their full atomic values. *Only peak-positions are relevant.* The best agreement is obtained at 60% scaling of  $CI(5f-6f)$ . Variation of the high-energy dipole peak position with varying scaling of : (b)  $CI(5f-6f)$ , and (c)  $(F_{df}^k, G_{df}^k)$ . While the latter shows a simple linear trend, the former shows a parabolic behavior with signs of saturation.

base of Fig. 1(a) (vertical scale not to be compared with the actual spectra above) clearly show that it also reproduces the mild shift of the HM peak at  $\sim 93$  eV, due to a  $q$ -dependent weight transfer between the  $l=3$  and  $l=5$  channels, as seen in experiments [17]. The dipole states, in general, mix much more and respond much more sensitively to the CI than the HM states. This also means that there is a substantial amount of interference between the  $5f$ -like and  $6f$ -like dipole transitions.

The origin of the higher sensitivity of the dipole compared to the HM is explained schematically in Fig. 1(b). Before CI (*left*), the difference ( $\Delta E$ ) in the CG energies for the two multiplets,  $5d^9 5f^1$  (width  $W_{mult}$ ) and  $5d^9 6f^1$  (width  $w_{mult}$ ), is  $\sim 23$ -24 eV, from H-F calculations. Although both the multiplets involve exactly the same terms,  $W_{mult}$  ( $\sim 25$  eV) is much larger than  $w_{mult}$  ( $\sim 7$  eV), demonstrating the difference between states involving the *same* versus *different principle quantum numbers*. Also, for a less-than-half-filled system with a low  $J$  ground state ( $J=0$  for  $\text{ThO}_2$ ), the highest multiplets (*red*) are generally *dipole-allowed*, while the lowest ones (*blue*) are the *HM-allowed* terms. Now  $CI(5f-6f)$  only mixes terms of the same symmetry [16], *e.g.*, the

*red* (*blue*) states at the *top* (*bottom*) of  $5d^9 5f^1$ , mix only with the *red* (*blue*) states at the *top* (*bottom*) of  $5d^9 6f^1$ . The result after mixing is shown in the *right panel*. Since  $w_{mult} \ll W_{mult}$ , the effective energy denominator for mixing of the *red* (*dipole*) terms is much smaller than that for the *blue* (*HM*) terms, causing the observed differences in the shifts. Due to these strong correlation effects, the effective “screening” becomes highly term dependent, explaining the strong asymmetry in the behavior of the dipole and the HM terms, which is not captured by a uniform reduction of the Slater integrals [17].

To show that the two approaches are qualitatively different, we compare in Fig. 2(a) the experimental  $q$ -averaged NIXS (*topmost*), with the calculated sum of the three component spectra ( $l=1, 3$  and  $5$ ), keeping  $(F_{df}^k, G_{df}^k)$  fixed at their atomic values, while the  $CI(5f-6f)$  are switched on and gradually increased to their atomic value (100%) (*top to bottom*). For this purpose only the peak positions are relevant. As already noted, a good agreement with HM peak positions is obtained for 60% reduction of  $CI(5f-6f)$ . But more importantly, with gradual uniform reduction in  $(F_{df}^k, G_{df}^k)$  we would expect a linear movement of the dipole towards the HM features. On the other hand with changing degree of CI, the dipole moves towards the HM peaks in a non-linear manner, showing signs of saturation, as governed by *level-repulsion physics*. This contrasting behavior is shown in Figs. 2(b) and 2(c), where we have plotted the dipole peak position in the two cases, as a function of the scaling of  $(F_{df}^k, G_{df}^k)$  and of  $CI(5f-6f)$ , respectively.

We now turn to the problem of the experimentally observed low relative amplitude, large width and non-lorentzian line shape of the GDR. This can be understood on the basis of Figs. 3(a)-(b). Fig. 3(a) shows the NIXS final state,  $5d^9 5f^{n+1}$ , of a  $5f^n$  actinide system. In the absence of the  $5d$  core-hole, this would be identical to the inverse photoemission final state  $5f^{n+1}$  (dashed line), and lies just below or within a continuum (shaded). Primarily, the core-hole provides an attractive scalar potential,  $Q$ , which is often large enough to pull down the  $5d^9 5f^{n+1}$  state, out of the continuum, forming a bound *core-hole exciton*. However, in a more complete picture (Fig. 3(b)), the core-hole  $f$ -electron multipole interaction, also yields a very broad multiplet structure (width  $W_{mult}$ ) about the CG of  $5d^9 5f^{n+1}$ . The Slater integrals are very large for these transitions occurring within the same  $n$ -shell, implying  $W_{mult} \gg Q$ . Thus while the HM states towards the bottom of the multiplet, still form bound states, the high-lying dipolar terms are pushed up into the continuum, offsetting the effect of  $Q$ , and their mixing gives rise to the GDR with characteristic Fano lineshapes, as seen experimentally. This physical picture clearly demonstrates why the dipole and the HM states show a crossover from V-B to bound character, in the  $5d \rightarrow 5f$  (actinides) [17], the  $4d \rightarrow 4f$  (RE compounds) [11], or the  $3p \rightarrow 3d$  (TM compounds) edges [14].

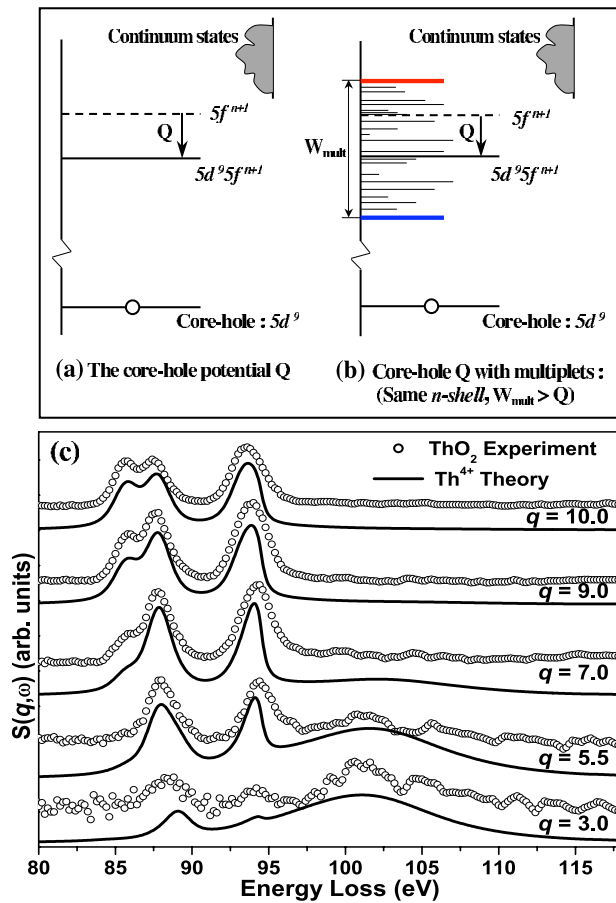


FIG. 3: (color online) Schematics showing (a) the effect of a scalar core-hole potential ( $Q$ ) on the NIXS final state; and (b) its fanning out due to strong core-valence multiplet effects leading to a gradual change from bound-states (lower terms) to V-B resonances (higher terms) as a function of energy; (c) the  $S(q, \omega)$  from a model calculation for  $\text{Th}^{4+}$  (lines) including a Fano-effect of the mixing of the atomic  $5d$ - $5f$  transition with that to a fictitious broad band, causing a broad, asymmetric lineshape of the high energy dipole term, that agrees well with experimental  $q$ -dependent NIXS for  $\text{ThO}_2$  [17] (symbols).

In Fig. 3(c) we show  $S(q, \omega)$  from a model calculation for  $\text{Th}^{4+}$  (lines) that includes transitions from the  $5d$  core-level to both the ( $5f, 6f$ ) levels as before (allowed  $l=1, 3, 5$ ), and to a fictitious  $7p$ -like discretized band (allowed  $l=1, 3$ ). The band is so positioned that it starts below the high energy dipole state, but above the HM states. The  $l=1, 3$  channels can interfere *via* the  $CI(5f-7p)$  matrix elements [20, 22]. We find that while the lower lying  $l=3, 5$  peaks remain sharp and excitonic, the high-energy dipole feature forms a GDR, just as discussed above. Interestingly, a dipole-allowed peak present at lower energy ( $\sim 88$  eV) is not broadened by this mechanism, implying that *the position within the multiplet, rather than the symmetry of the state, decides its fate*. A fairly good comparison with the experimental  $q$ -dependent NIXS for  $\text{ThO}_2$  [17] (symbols) is obtained if we use a somewhat larger Lorentzian width for the GDR

than the HM states, in order to simulate the multiplet dependent core-hole decay probabilities, not included in the present calculation. It is important to note that this dichotomy, between the dipole and the HM, could be reversed in cases where the dipole allowed states are lower in energy than the HM, like for more-than-half-filled systems which have large ground state  $J$  values [22].

In conclusion, the modeling of *same n-shell* NIXS is complicated by the simultaneous presence of V-B and bound states within the same final-state multiplet. The complex V-B resonances, involving non-local effects, provide insight into the hybridization of the locally excited core-electron with continua, and about core-hole decay processes. The dipole-forbidden bound states (not prominent in XAS) are modeled using a local, atomic CI approach, that provides direct ground state information. It also explains the apparent strong reduction of the atomic Slater integrals, which effectively become term dependent. The HM transitions and especially their angular dependence in single crystal studies [12, 13] are also expected to provide detailed information on the importance of “orbital-ordering” in the ground state and changes at phase transitions in “hidden order” materials like  $\text{URu}_2\text{Si}_2$  [3]. The V-B resonances are modeled with an additional term, mixing the  $5f$  states with a conduction band continuum, resulting in their broad and Fano-like line shapes. More realistic approaches to the latter would include an energy-dependent hybridization with a realistic density of states, and explicit core-hole decay processes. This is a topic of future investigations.

SSG and GAS acknowledge funding from the Canadian agencies NSERC, CFI and CIFAR. GTS and JAB acknowledge support from University of Washington, and the U.S. Department of Energy.

\* Electronic address: subhra@phas.ubc.ca

- [1] K. T. Moore and G. van der Laan, *Rev. Mod. Phys.* **81**, 235 (2009).
- [2] S. S. Hecker, in *Challenges in Plutonium Science*, **Vol. II**, (Los Alamos Science, Los Alamos, 2000).
- [3] T. T. M. Palstra *et al.*, *Phys. Rev. Lett.* **55**, 2727 (1985); V. Tripathi *et al.*, *Nature Phys.* **3**, 78 (2007); K. Haule and G. Kotliar, *Nature Phys.* **5**, 796 (2009).
- [4] D. van der Marel and G. A. Sawatzky, *Phys. Rev. B* **37**, 10674 (1988).
- [5] *Core Level Spectroscopy of Solids*, by F. de Groot and A. Kotani, CRC Press (Taylor & Francis Group, 2008).
- [6] U. Fano, *Phys. Rev.* **124**, 1866 (1961).
- [7] H. Ogasawara and A. Kotani, *J. Phys. Soc. Jpn.* **64**, 1394 (1995).
- [8] It is important to note that such a mechanism, relying on the coupling of the  $5d$  photoexcited state to the  $5f$  PES continuum *via* super-Coster-Kronig channels, is not operative for a  $5f^0$  system ( $\text{ThO}_2$ ) [9], as discussed here.
- [9] M. Richter *et al.*, *Phys. Rev. A* **39**, 5666 (1989).
- [10] G. Wendin, in *Giant Resonances in Atoms, Molecules*

- and Solids*, Vol. **151** of NATO Advanced Study Institute, Series B: Physics (Plenum, New York, 1987).
- [11] R. A. Gordon *et al.*, Europhys. Lett. **81**, 26004 (2008).
  - [12] B. C. Larson *et al.*, Phys. Rev. Lett. **99**, 026401 (2007).
  - [13] M. W. Haverkort, A. Tanaka, L. H. Tjeng, and G. A. Sawatzky, Phys. Rev. Lett. **99**, 257401 (2007).
  - [14] R. A. Gordon, M. W. Haverkort, Subhra Sen Gupta and G. A. Sawatzky, J. Phys.: Conf. Ser. **190**, 012047 (2009).
  - [15] *Electron Dynamics by Inelastic X-Ray Scattering* by W. Schuelke, Oxford University Press (2007).
  - [16] *The Theory of Atomic Structure and Spectra* by R. D. Cowan, University of California Press (1981).
  - [17] For details see the companion paper : J. A. Bradley *et al.* (*submitted to PRL*).
  - [18] E. Antonides, E. C. Janse and G. A. Sawatzky, Phys. Rev. B **15**, 1669 (1977); *ibid.* **15**, 4596 (1977).
  - [19] B. T. Thole *et al.*, Phys. Rev. B **32**, 5107 (1985); H. Ogasawara *et al.*, Phys. Rev. B **44**, 2169 (1991).
  - [20] In our case, the  $CI(\alpha-\beta)$  matrix elements refer to the Slater Coulomb and exchange integrals  $R^k(5d, \alpha, 5d, \beta)$ .
  - [21] A. Tanaka and T. Jo, J. Phys. Soc. Jpn. **63**, 2788 (1994).
  - [22] *Details in* Subhra Sen Gupta *et al.* (*to be submitted*).